0026-895X/96/050842-10$3.00/0

MOLECULAR PHARMACOLOGY, 49:842–851 (1996).

Selective Inhibition of Topoisomerase II by ICRF-193 Does Not Support a Role for Topoisomerase II Activity in the Fragmentation of Chromatin during Apoptosis of Human Leukemia Cells

HELEN M. BEERE, CHRISTINE M. CHRESTA, and JOHN A. HICKMAN

Cancer Research Campaign Molecular and Cellular Pharmacology Group, School of Biological Sciences, University of Manchester, Manchester, UK M13 9PT

Received June 28, 1995; Accepted February 5, 1996

SUMMARY

Specific inhibitors of topoisomerase II (e.g., ICRF-193, an inhibitor of the catalytic activity of topoisomerase II and etoposide that stabilizes enzyme/DNA cleavable complexes) have been used to probe the role of topoisomerase II in the fragmentation of DNA during drug-induced apoptosis of human HL-60 leukemia cells. Topoisomerase II plays a role in the attachment of 50-kilobase domains of DNA to the nuclear matrix; fragments of this size are cleaved during apoptosis. Apoptosis was induced by 50 μM etoposide or 300 mM *N*-methylformamide (NMF), a nongenotoxic agent. Treatment with etoposide or NMF induced the morphology of apoptosis within 4 hr. Analysis of DNA integrity by electrophoresis showed coincident fragmentation from 50 kb and to integers of 200 bp. Transient protein-associated DNA strand breaks, characteristic of etoposide-induced damage, were visualized as DNA fragments of >600 kb. Preincubation with ICRF-193 (100 μM) reduced the number of etoposide-induced DNA strand breaks by 50% and delayed the appearance of DNA fragmentation by ~18 hr. However, ICRF-193 had no effect on either NMF- or camptothecin-induced DNA fragmentation. The induction of apoptosis by both etoposide and NMF was associated with a reduction in the cellular levels of topoisomerases IIα and IIβ. ICRF-193 inhibited proteolytic cleavage of topoisomerase II induced by etoposide but not by NMF. The data suggest that the activity of topoisomerase II is not required for the cleavage of DNA to 50-kb fragments but that proteolysis of topoisomerase II represents a conserved event of apoptosis.

Biochemical events leading to an apoptotic cell death are of two classes: those that may act as initiating events, or "triggers," and those that effect the commitment to death. The nature of the effector(s) is uncertain. This uncertainty is a reflection of the scant knowledge of biochemical events that enact a morphologically highly conserved pattern of cell death. It is presumed, however, that the biochemical effector mechanisms may also be highly conserved. Which of these biochemical events, represented by chromatin condensation and cytoplasmic changes, irreversibly commits the cell to a programmed cell death remains unanswered, but clearly extensive DNA fragmentation constitutes a fatal lesion.

The early dogma that internucleosomal DNA cleavage is the biochemical event responsible for the appearance of condensed chromatin (1) has been challenged by us and others (2–5). Accumulating evidence suggests that the changes in nuclear morphology observed during apoptosis seem to be more closely correlated with the onset of higher-order chromatin fragmentation, an event that has been shown to precede (4, 6–7), or, in some cell types, to occur in the absence of (3, 5, 8) internucleosomal DNA cleavage. Analysis of DNA integrity in a variety of cells, including thymocytes (6, 9), lymphocytes (10), and several epithelial cell types (3), has demonstrated the generation of discrete DNA fragments of ~50 and ~300 kb during apoptosis induced by a variety of stimuli. The question remains of how such higher-order fragments of DNA of chromatin are formed.

Topoisomerase II catalyzes the ATP-dependent transient breakage and resealing of double-stranded DNA (11) and is a major constituent of nuclear matrices isolated from interphase nuclei and metaphase chromosomes (12, 13). Immunolocalization studies showing it to be situated at the base of chromatin loops (14) and demonstration of specific interaction between topoisomerase II and DNA containing scaffold attachment regions (15) suggest a structural role for topoisomerase II in the anchorage of chromatin to the nuclear

This research was supported by Cancer Research Campaign Grants SP1518 (J.A.H.) and SP2234 (C.M.C.).

ABBREVIATIONS: NMF, *N*-methylformamide; CPT, camptothecin; FIGE, field inversion gel electrophoresis; SSB, single-strand breaks; bp, base pair(s).

matrix. Scaffold attachment regions are also highly enriched in sequences homologous to the topoisomerase II cleavage consensus sequence (16, 17).

Filipski *et al.* (18) reported that nuclease digestion of DNA from isolated nuclei yielded discrete fragments of ~50 and ~300 kb. They postulated that the 50-kb fragmentation pattern reflected chromatin loop organization, whereas a 300-kb periodicity resulted from cleavage of groupings of these loops that form a higher-order chromatin structure. Treatment of thymocytes with topoisomerase II poisons resulted in the same pattern of chromatin cleavage. This could be reversed by reincubation of the cells in drug-free medium, suggesting that topoisomerase II may enzymatically cleave the DNA at the base of loops. However, we recently showed that the ends of the 50-kb DNA fragments, formed during apoptosis, were not associated with protein (5). The coincident proteolysis of topoisomerase II that we observed may account for the potential loss of topoisomerase II from the ends of these DNA fragments (5). We now approached the determination of the involvement of topoisomerase II in apoptosis by using specific inhibitors of the activity of topoisomerase II.

Etoposide is a nonintercalative topoisomerase II poison that induces protein-associated DNA strand breaks through stabilization of the covalently linked topoisomerase II/DNA cleavable complex (19, 20). In contrast, inhibition of topoisomerase II by ICRF-193 and other bis(dioxopiperazine) derivatives (21) is characterized by direct interaction and attenuation of the catalytic activity of the enzyme in the absence of cleavable complex formation (22). Recent studies have also shown that ICRF-193 and related compounds inhibit the formation of DNA/protein cross links and cytotoxicity induced by a variety of topoisomerase II poisons, including etoposide, *m*-amsacrine, and Adriamycin (23).

The use of topoisomerase II-specific poisons alone for the study of mechanisms involved in the degradation of DNA during apoptosis is complicated by the superimposition of the DNA breaks arising directly from the inhibition of topoisomerase II activity and those initiated as a consequence of the activation of apoptosis. In a recent study, we showed that the DNA cleavage pattern induced by etoposide differed with respect to cleavage induced by the drug (>600-kb fragments) and to that representative of the apoptotic process itself (300- and 50-kb fragments). We therefore also used NMF as an agent that rapidly induces apoptosis of human leukemia cells (5, 24) but does not directly induce DNA damage or interact with topoisomerase II to investigate a role for topoisomerase II in the DNA fragmentation associated with apoptosis.

Experimental Procedures

Materials

All materials were obtained from Sigma Chemical Co. (Poole, Dorset, UK) unless otherwise stated. Anti-topoisomerase α and β monoclonal antibodies were very generous gifts from Dr. F Drake (Smith, Kline and Beecham, Herts, UK) and Dr. Ian Hickson (ICRF, Oxford, UK), respectively. ICRF-193 was kindly provided by Dr. Andrew Creighton (ICRF, London, UK). Anti-bcl-2 antibody was purchased from Dako Limited (High Wycombe, Bucks, UK).

Cell Culture

HL-60 human promyelocytic leukemia cells (25) were maintained in RPMI-1640 medium (Imperial Laboratories, Andover, Hampshire, UK) supplemented with 2 mM L-glutamine and 10% fetal calf serum (Advanced Protein Products) at 37° in an atmosphere of 95% air/5% CO_2 with 100% humidity. Cells were routinely maintained in logarithmic phase growth between 1×10^5 and 1×10^6 cells/ml by biweekly subculture and had an approximate doubling time of 24 hr. Stock cultures of HL-60 cells were maintained for ~20 passages before reestablishment from frozen, banked cultures and were regularly tested to ensure that they were free of *Mycoplasma* contamination. NMF, etoposide, CPT, or ICRF-193 was added to cells in the logarithmic phase of growth. Cell samples were removed at predetermined time points for the assessment of DNA integrity or for protein or flow cytometric analyses.

Detection of DNA Fragmentation

Conventional gel electrophoresis. Cells (10^6) were resuspended in 20 μl of lysis buffer (10 mM EDTA, 50 mM Tris·HCl, pH 8, 0.5% sodium lauryl sarcosinate, and 0.5 mg/ml proteinase K) and incubated for 1 hr at 50°. RNase A was added (10 μl at 0.5 mg/ml), and the incubation was continued for 1 additional hr at 50°. After the addition of 10 μl of 10 mM EDTA, pH 8, containing 1% low temperature gelling agarose, cell samples were loaded into dry wells of a 2% agarose gel stained with ethidium bromide (0.5 μg/ml). Samples were allowed to solidify for 5 min before the gel was flooded with TPE buffer (0.09 M Tris-phosphate, 0.002 M EDTA) and subjected to electrophoresis at 40 V for 3–4 hr. DNA was visualized with a UV transilluminator.

FIGE. FIGE was performed as we described previously (5) as a modification of the method of Filipski *et al.* (18).

Immunoblotting. Immunoblotting was performed as detailed previously (5). Briefly, cells were sonicated on ice to lyse the cells and disrupt the nuclear matrices, and DNase was added to each sample to prevent the retardation of topoisomerase II by etoposide-induced DNA/protein complexes. The protein content of each whole-cell extract was then estimated with the use of Bio-Rad protein assay reagent, and 75 μg of protein/lane was analyzed with sodium dodecyl sulfate-polyacrylamide gel electrophoresis (7% acrylamide resolving gel/4% acrylamide stacking gel). After the electrophoretic transfer of proteins to nitrocellulose Immobilon-P PVDF membrane (50 mM CAPS, pH11), gels were stained with Coomassie blue to visualize remaining protein and to ensure that the gels had been equally loaded. Topoisomerase IIα was detected with affinity purified antibody raised against a dodecapeptide specific to human topoisomerase IIα (p170) (26) and topoisomerase IIβ (p180) with the mouse monoclonal 8D7 (27). Immunodetection of bcl-2 protein also acted as a control for equal loading. The antibody-specific proteins were visualized using the enhanced chemiluminescence detection system (Amersham, Buckinghamshire, UK) according to the manufacturer's instructions.

Alkaline Elution

DNA SSBs were measured with alkaline elution (pH 12.1) as described previously (28). Early logarithmic phase HL-60 cells (2×10^5/ml) were labeled for 24 hr with 0.015 μCi/ml [^{14}C]thymidine (specific activity, 56 μCi/mmol; Amersham), centrifuged, and resuspended in fresh medium at 2×10^5 cells/ml for 2 hr before drug exposure. After drug treatment, cells were collected by centrifugation and resuspended in ice-cold phosphate-buffered saline. Cells (8×10^5) were loaded onto each filter and rinsed with 10 ml ice-cold phosphate-buffered saline before lysis. For measurement of DNA SSBs, cells were lysed with a sarcosyl lysis solution (0.2% sodium dodecyl sarcosine, 2 M NaCl, 0.04 M EDTA, pH 10) onto 2 μM polycarbonate filters (Millipore). DNA was eluted for 15 hr at 0.04 ml/min with tetraethylammonium hydroxide, pH 12.1, containing 0.1% sodium dodecyl sulfate. DNA remaining on the filter and in the filter funnels was released as described previously (28). The frequency of SSBs induced by etoposide was converted to rad equivalents using a calibration graph derived from the number of SSBs produced by a known X-ray dose.

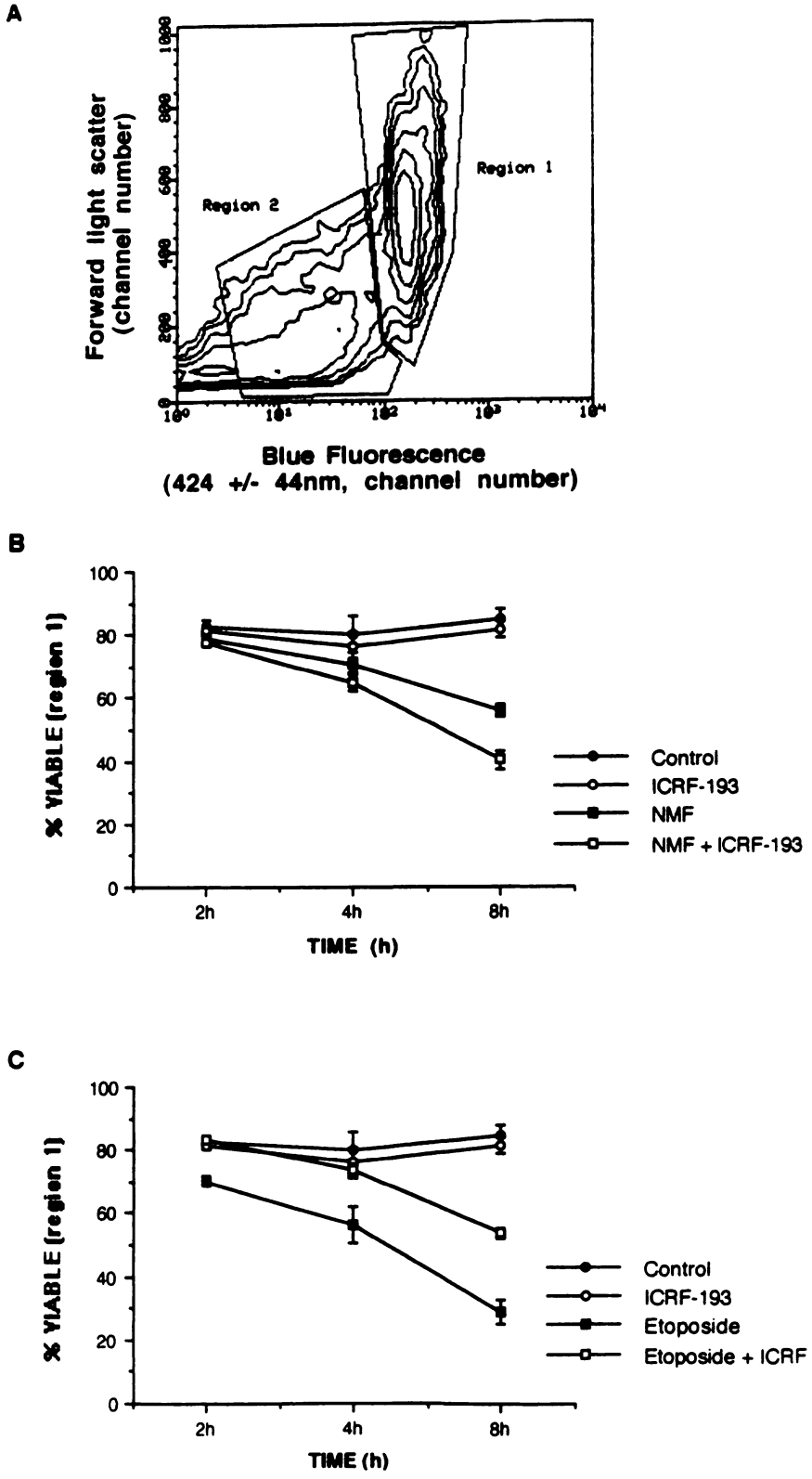

Fig. 1. Flow cytometric analysis of apoptosis in nonfixed HL-60 cells with Hoechst 33342 and propidium iodide. Representative two-dimensional frequency contour plot of blue Hoechst-DNA fluorescence versus forward light scatter (cell size) (A) after an 8-hr exposure of cells to etoposide (50 μM). We excluded cellular debris and red propidium fluorescence for the purpose of data analysis. Morphological analysis confirmed that cells in region 2 exhibited features characteristic of apoptosis (condensation and fragmentation of chromatin). Those cells in region 1 were morphologically indistinguishable from untreated viable cells. Both drugs induced a time-dependent decrease in cell viability. Analysis of the number of cells in region 1 after exposure to 300 mM NMF (B) or 50 μM etoposide (C) in the presence and absence of 100 μM ICRF-193 showed that the etoposide-induced loss in cell viability was reduced in the presence of ICRF-193. In contrast, the number of cells in region 1 after exposure to NMF was unaffected by pretreatment with ICRF-193. B and C, Mean data ± standard deviation from three independent experiments.

Flow Cytometric Analysis

Analysis of the kinetics of apoptosis was determined according to a previously published flow cytometric method (29). Approximately 5 × 10^5 cells in 1 ml of medium were removed at predetermined time points after drug addition (±ICRF-193). Hoechst 33342 was added to each of the unfixed samples to a final concentration of 10 μM and incubated for 5 min at room temperature. Samples were then stained with 10 μl of propidium iodide (3.2 mg/ml) for 1–2 min before flow cytometric analysis with a Becton Dickinson FACS Vantage instrument (San Jose, CA) equipped with a Coherent Enterprise laser set to excite at 60 mW using the 337 nm line. Forward light scatter, blue fluorescence (Ho342/DNA, log scale, 424 ± 44 nm), and red fluorescence (propidium/DNA, linear scale, 575 ± 22 nm) were measured for each sample at a flow rate of 300–500 cells/sec. Data were analyzed

as two-dimensional frequency contour plots of forward light scatter versus log blue fluorescence after exclusion of cell debris and red fluorescent events (PC-LYSIS software, Hewlett-Packard). Cell populations were also sorted based on blue fluorescence intensity, and the morphology was assessed with the use of fluorescence microscopy (29).

Results

Analysis of the kinetics of apoptosis. We first established the kinetics of apoptosis in response to a range of concentrations of NMF and etoposide by using a flow cytometric assay (29) (data not shown). For a more detailed study, we then selected a single concentration of each agent (300 mM NMF or 50 μM etoposide) that induced significant levels of apoptosis in the absence of necrosis. Fig. 1A shows representative data expressed as a two-dimensional frequency contour plot of forward light scatter (cell size) versus log blue Hoechst fluorescence (reflecting DNA content) collected from the analysis of HL-60 cells after an 8-hr exposure to etoposide. To set the parameters for analysis, the data obtained were first expressed as a forward versus orthogonal light scatter plot, and a primary gate was positioned to exclude cellular debris. Typically, ~5% of the total events recorded for untreated cells were excluded. The percentage debris increased to ~20% under conditions shown to induce significant levels of apoptosis. Of those events included within the first gate, the percentage exhibiting red fluorescence (indicative of a permeable plasma membrane) was also excluded and typically represented <2% of the total population under each of the conditions examined. The remaining population was then expressed as a two-dimensional frequency contour plot of forward light scatter versus log blue Hoechst fluorescence, as shown in Fig. 1A. Additional gates were positioned to define the viable cell subpopulation (region 1) and that containing events showing significantly reduced blue Hoechst fluorescence and forward light scatter (region 2). These events represent predominantly apoptotic cells, although DNA-containing apoptotic bodies may also be included. Fluorescence-activated sorting of these two subpopulations and assessment of their morphology through the fluorophore acridine orange and fluorescence microscopy (29) showed that events within population 2 exhibited morphological features characteristic of apoptosis, including condensation and fragmentation of chromatin (data not shown). Statistical analysis of the data collected was then expressed in graphic form to show the percentage of viable cells within region 1 (Fig. 1, B and C) after treatment of cells with 300 mM NMF and 50 μM etoposide in the presence and absence of ICRF-193 (Fig. 1, B and C, respectively). The onset of etoposide-induced apoptosis slightly preceded that induced by NMF, with a significant increase above control level evident by 2 hr (Fig. 1C). We then determined the effect of a range of

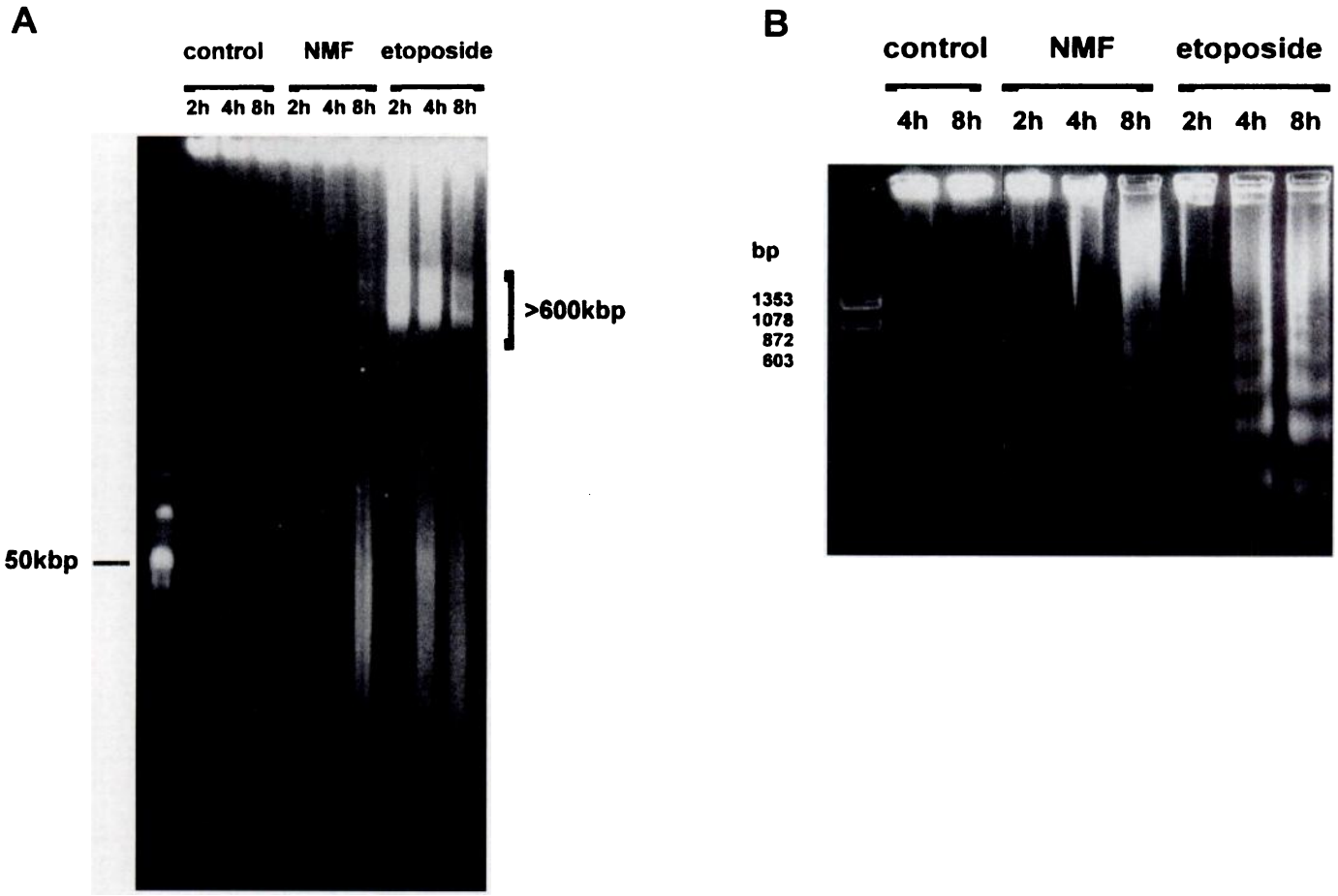

Fig. 2. DNA fragmentation associated with NMF- or etoposide-induced apoptosis. FIGE of DNA isolated from untreated HL-60 cells (*lanes 2–4*) and those exposed to 300 mM NMF (*lanes 5–7*) or to 50 μM etoposide (*lanes 8–10*) (A). DNA markers are shown in *lane 1*. DNA fragmentation in response to both agents was observed from ~50 kb. Conventional gel electrophoresis showed internucleosomal DNA fragmentation (NMF, *lanes 4–6*; etoposide, *lanes 7–9*) (B).

concentrations (50–200 μM) of the topoisomerase II inhibitor ICRF-193 on apoptosis induced by NMF or etoposide (data not shown) and a single concentration of ICRF-193 selected for further study. Data in Fig. 1C show that preincubation with 100 μM ICRF-193 significantly inhibited etoposide-induced apoptosis, although it was one of delay rather than complete abrogation. In contrast, preincubation of cells with ICRF-193 had no effect on NMF-induced apoptosis (Fig. 1B).

Induction by NMF and etoposide of DNA fragmentation from ~50 kbp. With the use of FIGE, the pattern of higher-order chromatin fragmentation was determined in response to 300 mM NMF and 50 μM etoposide (Fig. 2A). Exposure of cells to 300 mM NMF induced the appearance of a specific pattern of DNA degradation (*lanes 5–7*): evidence of fragmentation to ~50 kb was just visible by 4 hr but was clearly increased after 8 hr of drug treatment (*lanes 6 and 7*, respectively). This correlates closely with the kinetics of the onset of apoptosis determined through flow cytometric analysis (Fig. 1B). Incubation of cells with 50 μM etoposide induced a similar DNA cleavage pattern to produce fragmentation from 50 kb that slightly preceded that induced by NMF. In addition, a larger DNA band of >600 kb was observed that was clearly visible before the detection of 50-kb fragmentation (*lane 8*) and was seen to progressively decrease with time (*lanes 8–10*). Its transient appearance correlated with a progressive increase in the detection of fragmentation from 50-kb and to 200-bp DNA integers (see below). The >600-kb band was apparent only in cells treated with etoposide, not in cells exposed to NMF. The appearance of DNA fragmentation from 50 kb was coincident with the

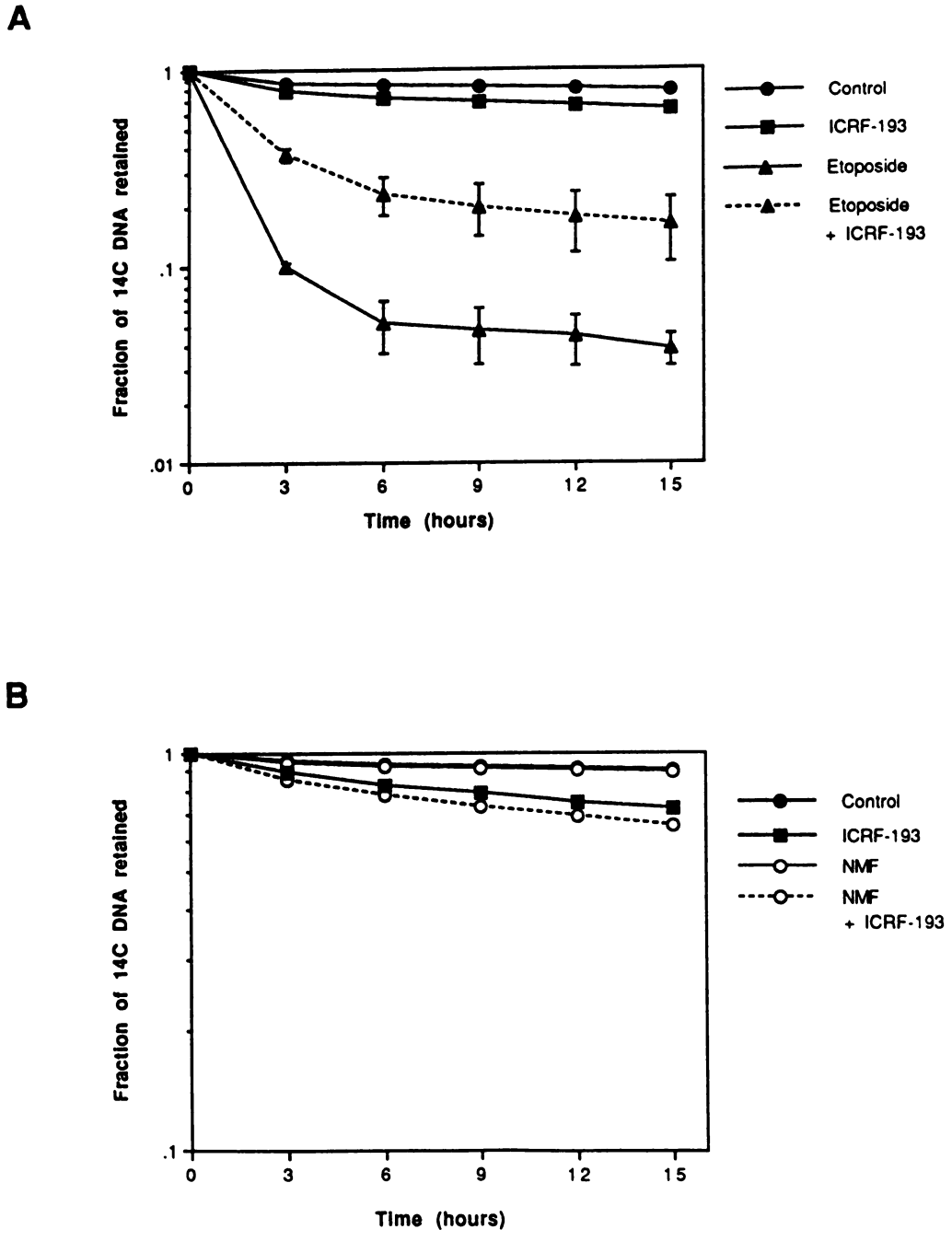

Fig. 3. The effect of the topoisomerase II inhibitor ICRF-193 on the induction of DNA strand breaks by etoposide and NMF as measured with alkaline elution analysis. HL-60 cells were preincubated with ICRF-193 (100 μM) for 1 hr before exposure to etoposide (50 μM) (A) or NMF (300 mM) (B) for 1 additional hr before analysis with alkaline elution. Protein-associated DNA breaks, induced by etoposide, were significantly reduced in the presence of ICRF-193. No effect of NMF on DNA integrity at ≤15 hr after the initial 1-hr exposure period was detected with alkaline elution analysis.

detection of internucleosomal DNA cleavage to integers of 200 bp in response to both etoposide and NMF (Fig. 2B).

Inhibition by ICRF-193 of the induction of etoposide-induced DNA SSBs. Cells were pretreated with ICRF-193 (100 μM) for 1 hr before the addition of etoposide (50 μM) and were then incubated in the presence of etoposide for 1 additional hr before analysis by alkaline elution. ICRF-193 pretreatment reduced the number of DNA SSBs induced by etoposide (Fig. 3A); DNA damage (in rad equivalents) decreased from 565 for etoposide alone to 290 in the presence of ICRF-193, a reduction of ~50%. ICRF-193 induced a small increase in SSBs (60 rad equivalents) compared with control. NMF alone did not produce DNA SSB and did not alter the frequency of SSBs induced by ICRF-193 (Fig. 3B), confirming its nongenotoxic mechanism of action.

Inhibition by ICRF-193 of etoposide- but not NMF- or CPT-induced 50-kb DNA fragments. Cells were preincubated for 1 hr with 100 μM ICRF-193 before the addition of either 300 mM NMF, 1 μM CPT, or 50 μM etoposide, and the integrity of DNA was analyzed with FIGE. Preexposure of cells to ICRF-193 before incubation with etoposide inhibited the DNA fragmentation from 50 kb and to fragments corresponding to >600 kb at ≤12 hr after drug treatment (Fig. 4A, *lanes 13–16*). However, there was evidence of DNA fragmentation after a 24-hr exposure to etoposide in the presence of ICRF-193 (Fig. 4A, *lane 16*). Incubation with ICRF-193 alone had no detectable effect on DNA integrity for ≤24 hr, after which some fragmentation was observed (Fig. 4, A, *lanes 5–8*, and C, *lane 3*). The kinetics of etoposide-induced fragmentation from 50 kb in the presence and absence of ICRF-193 (Fig. 1) was paralleled by data showing ICRF-193-mediated suppression of etoposide-induced internucleosomal DNA cleavage (Fig. 5A, *lanes 10–13*). In contrast, preincubation of cells with ICRF-193 had no inhibitory effect on NMF-induced DNA fragmentation from 50 kb (Fig. 4B, *lanes 5–12*) or on internucleosomal DNA fragmentation (Fig. 5B, *lanes 8–15*). Preexposure of cells to ICRF-193 was shown to have no effect on the pattern of CPT-induced DNA fragmentation to high molecular weight fragments (Fig. 4C) or on internucleosomal cleavage stimulated by the inhibition of topoisomerase I (Fig. 5C), confirming the specificity of the ICRF-193 inhibition of topoisomerase II-mediated cleavage of DNA.

Inhibition of etoposide- but not NMF-induced topoisomerase II degradation by ICRF-193. Representative Western blot analyses of the levels of topoisomerase IIα and IIβ proteins in whole-cell extracts after exposure to either NMF or etoposide are shown in Fig. 6. After exposure of cells to 300 mM NMF, the level of topoisomerase IIα (Fig. 6) had decreased significantly by 8 hr (*lane 9*). Evidence of a slight decrease was observed by 4 hr (*lane 8*). Etoposide also induced a time-dependent decrease in the level of topoisomerase IIα protein (*lanes 4–6*) that, like the appearance of DNA fragmentation (Fig. 2), slightly preceded that observed with NMF. The level of topoisomerase IIβ protein was shown to decrease in response to both agents (Fig. 6), although less rapidly than that observed for topoisomerase IIα. The level of

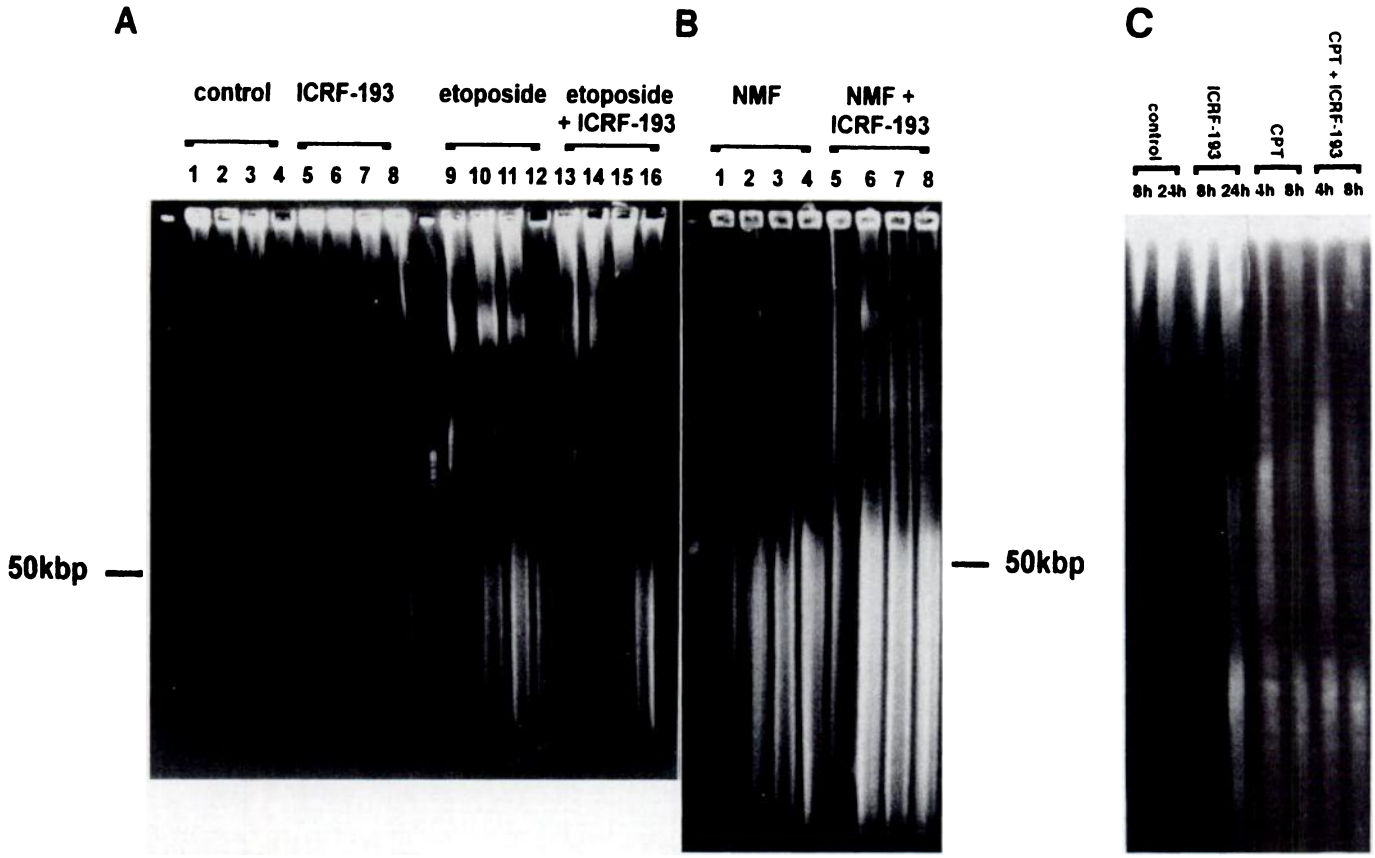

Fig. 4. The effect of the topoisomerase II inhibitor ICRF-193 on higher-order DNA fragmentation. HL-60 cells were preincubated with ICRF-193 (100 μM) for 1 hr before exposure to etoposide (50 μM) (A), NMF (300 mM) (B), or CPT (1 μM) (C) and analysis by FIGE. ICRF-193 significantly delayed the onset of etoposide-induced 50-kb fragmentation (A, *lanes 9–16*). Neither NMF- (B, *lanes 1–4*) nor CPT- (C, *lanes 5 and 6*) induced 50-kb fragmentation was affected by ICRF-193 (B, *lanes 5–8*; C, *lanes 7 and 8*).

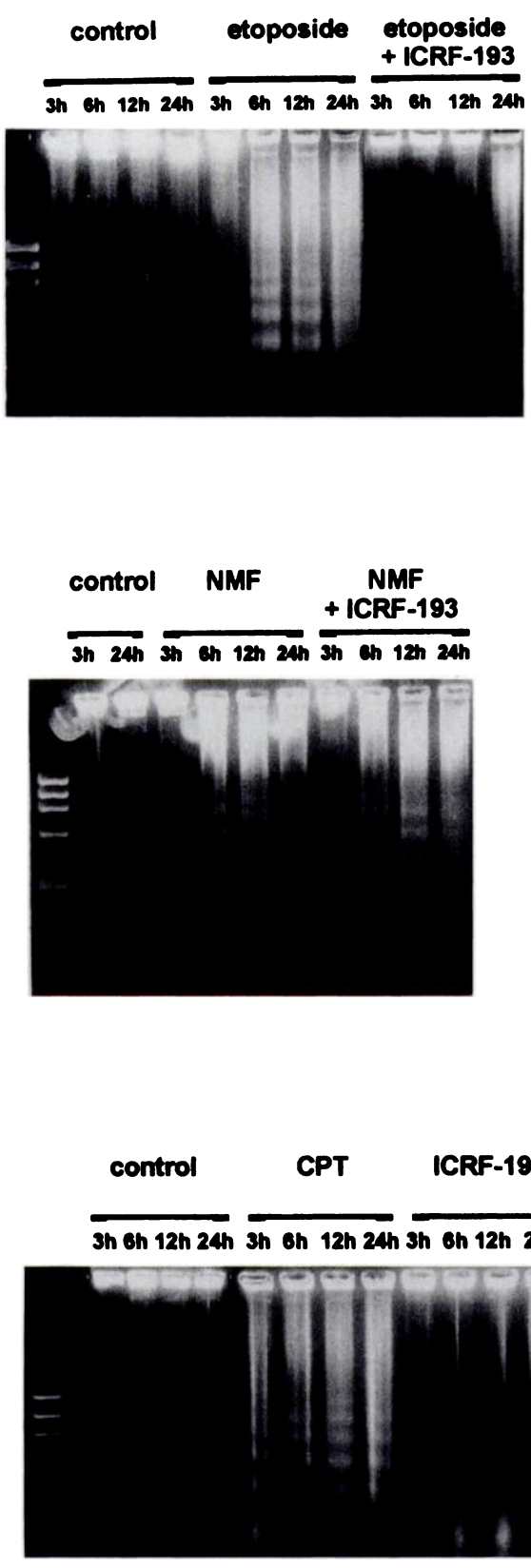

Fig. 5. The effect of the topoisomerase II inhibitor ICRF-193 on internucleosomal DNA cleavage. HL-60 cells were preincubated with ICRF-193 (100 μM) before treatment with 50 μM etoposide (A) or 300 mM NMF (B) and analysis with electrophoresis. ICRF-193 significantly delayed the onset of etoposide-induced internucleosomal DNA cleavage (A, *lanes 10–13*). In contrast, NMF-induced internucleosomal DNA fragmentation (B, *lanes 4–7*) was unaffected by ICRF-193 (B, *lanes 8–11*). Internucleosomal DNA fragmentation, induced by the topoisomerase I inhibitor, CPT (C) was also unaffected by a preincubation with ICRF-193 (C, *lanes 14–17*).

bcl-2 protein was unchanged in response to both agents throughout the duration of the experiment, confirming equal loading of protein.

We next examined the effect of ICRF-193 on NMF- and etoposide-induced topoisomerase II degradation. Fig. 7 shows representative immunoblots for topoisomerases IIα and IIβ after exposure to NMF or etoposide in the presence and absence of ICRF-193. Preincubation with ICRF-193 prevented the etoposide-associated decrease in the level of topoisomerase IIα protein (Fig. 7B, *lanes 9–11*). In contrast,

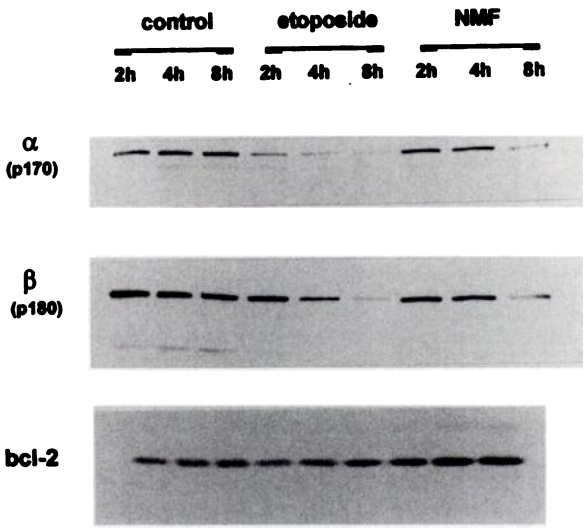

Fig. 6. Representative Western blot analysis of the levels of topoisomerase IIα (top) and IIβ (center) proteins after exposure of HL-60 cells to 50 μM etoposide (*lanes 4–6*) and 300 mM NMF (*lanes 7–9*). Both agents were shown to induce a time-dependent decrease in the levels of both topoisomerase II isoforms. In contrast, the level of bcl-2 protein remained unchanged (*bottom*), confirming equal loading of protein.

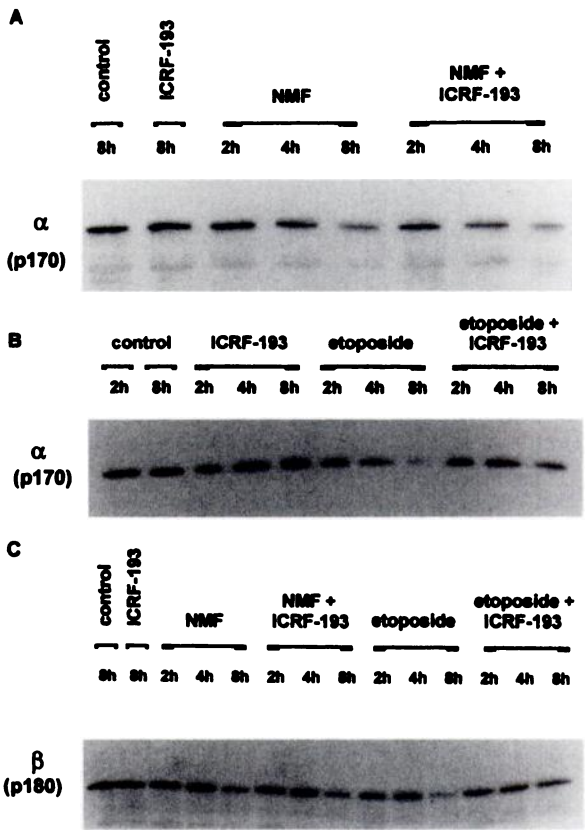

Fig. 7. Representative Western blot analysis of the levels of topoisomerase IIα (A and B) and IIβ (C) isoforms after treatment with either NMF or etoposide in the presence and absence of ICRF-193. HL-60 cells were preincubated with the topoisomerase II inhibitor ICRF-193 (100 μM) for 1 hr before treatment with 300 mM NMF or 50 μM etoposide. NMF induced a decrease in the level of both topoisomerase IIα (A, *lanes 3–5*) and IIβ (C, *lanes 3–5*) (also shown in Fig. 8, *lanes 7–9*) that was unaffected by a preincubation with ICRF-193 (A, *lanes 6–8*, and C, *lanes 6–8*). In contrast, preincubation with ICRF-193 before treatment of cells with etoposide was shown to abrogate the decrease in protein levels observed in the presence of etoposide alone (B, *lanes 9–11*, and C, *lanes 12–14*).

NMF-associated degradation of topoisomerase IIα was not prevented by the inclusion of ICRF-193 (Fig. 7A, *lanes 3–8*). Similar results were obtained from Western blot analysis for topoisomerase IIβ expression (Fig. 7C).

Discussion

An emerging model for the events that initiate apoptosis is one in which a proteolytic cascade may be activated in the cytoplasm; this then disseminates in some way to the nucleus where cleavage of DNA ensues (30). DNA cleavage and the associated condensation of chromatin may be key steps in the irreversible commitment of a cell to an apoptotic death. Our recent work (3, 5) and that of others (2, 4, 6) had shown that DNA cleavage yielded high molecular weight fragments before or even in the absence of internucleosomal DNA cleavage (1). These higher-order fragments of DNA may represent a stage integral with the appearance of condensed chromatin (3, 5–7).

The results presented here show that HL-60 cells undergo DNA degradation to ~50-kb fragments after both genotoxic and nongenotoxic challenge. Higher-order DNA fragmentation in this cell line is observed concomitant with the condensation of chromatin and internucleosomal DNA cleavage (Figs. 1 and 2). The data show that there is a coincident rather than sequential appearance of 50-kb and 180–200-bp integer fragmentation (Fig. 2, A and B). The coincidence of internucleosomal DNA cleavage with the cleavage of higher-order chromatin is reflected in the detection of DNA fragments of <50 kb (Fig. 2A) and the simultaneous laddering pattern (Fig. 2B). This contrasts with our previous study, in which MOLT-4 cells showed cleavage to discrete 50-kb fragments only and no ladder (5).

The appearance of DNA fragmentation from 50 kb suggests that domains of DNA may be cleaved at their anchorage points (for a review, see Ref. 30). There is evidence that topoisomerase II plays a structural role at these anchorage points (see introductory paragraphs). Topoisomerase II is also able to cleave DNA to produce a protein-associated double-strand break; an obvious question is whether topoisomerase II may be involved in the formation of higher-order fragments of DNA. Apoptosis in MOLT-4 cells, induced by etoposide or NMF, was associated with 50-kb DNA fragments. These fragments acted as substrates for terminal deoxynucleotidyltransferase, supporting the idea that DNA 3′-OH ends were not protein associated or occluded by topoisomerase II (5). However, because we observed that DNA cleavage was accompanied by the breakdown of topoisomerase II, it was possible that the 3′-OH ends became exposed after proteolysis of topoisomerase II. We have therefore used an inhibitor of the enzymatic activity of the topoisomerase II enzyme, ICRF-193, to probe the possible involvement of the enzyme in the release of 50-kb domains of DNA.

Preincubation of HL-60 cells with ICRF-193 was shown to inhibit etoposide-induced DNA damage by 50%, as determined through alkaline elution analysis (Fig. 3A). This is in agreement with earlier studies showing inhibition of etoposide-induced cleavable complex formation (22, 23, 31). ICRF-193 also inhibited the onset of etoposide-induced apoptosis,

as measured with flow cytometry (Fig. 1C), and the appearance of DNA fragmentation from 50 kb and internucleosomal DNA cleavage products (Figs. 4A and 5A, respectively). In contrast to etoposide-mediated DNA degradation, NMF-induced cleavage of DNA from 50 kb and to internucleosomal fragments was unaffected by pretreatment with ICRF-193 (Figs. 4 and 5). Similar data were obtained when we investigated the induction of apoptosis by the topoisomerase I inhibitor camptothecin (Fig. 4C). This suggests that the cleavage of DNA to 50-kb fragments does not require the enzymatic activity of topoisomerase II.

Exposure of HL-60 cells to etoposide also induced the formation of additional high molecular weight DNA fragment(s). These were visualized as an unresolved band of >600 kb before the detection of DNA fragmentation from 50 kb (Figs. 2A and 4A). The formation of this band was significantly reduced by preincubation with ICRF-193 (Fig. 4A). NMF-mediated DNA fragmentation was characterized by the absence of a >600-kb band (Figs. 2A and 4B), suggesting that it may be either a specific product of etoposide/topoisomerase II-induced damage or restricted to, and characteristic of, etoposide-induced apoptosis. This result is essentially the same as that observed during etoposide-induced apoptosis in MOLT-4 cells (5). This again raises questions regarding the location of topoisomerase II molecules on chromatin: stabilization of cleavable complexes by etoposide did not produce fragments of 50–80 kb, the suggested size of the topoisomerase II-attached "domains" (for a review, see Ref. 30), as might have been expected. The kinetics of the appearance of DNA fragments of >600 kb is therefore indicative of topoisomerase II-associated cleavable complex formation (10) (Fig. 3) at sites located a greater distance apart on chromatin than has been suggested. Inhibition of the formation of these breaks at >600 kb by ICRF inhibits both the subsequent DNA cleavage and the associated proteolysis of topoisomerase II.

What is the mechanism by which the 50-kb DNA fragments are generated if it does not involve topoisomerase II activity? NMF-induced apoptosis in the presence of ICRF-193 (Figs. 4B and 5B) does not support the idea that topoisomerase II is involved in the cleavage of DNA to ~50-kb fragments, nor does our previous work, in which we suggested that the 3′-OH ends of 50-kb DNA fragments were not protein associated (5), support the idea of an active role for topoisomerase II in the cleavage of DNA during apoptosis. However, the coincident degradation of topoisomerase IIα and IIβ proteins (Fig. 6) with the appearance of DNA fragmentation suggests that proteolysis of nuclear structural proteins (32) may facilitate some change in chromatin topology that promotes subsequent cleavage by endonuclease(s). The rapid proteolysis of lamins during apoptosis (33) has similarly been suggested to allow access of cytoplasmic enzymes, such as DNAse I, to the nuclear compartment, resulting in internucleosomal DNA cleavage (34, 35). The importance of proteolysis in the nonrandom cleavage of DNA during drug-induced apoptosis has also been demonstrated in both HL-60 cells and thymocytes (32, 35–37). Continued investigation into the role of cytoplasmic proteases in the initiation of nuclear changes may provide insight into the critical events determining a programmed loss of cell viability.

Acknowledgments

We thank Caroline Dive and Sukhbinder Heer for performing the flow cytometry experiments and Scott Kaufmann for advice and criticism. We are most grateful to Dr. Andrew Creighton for the generous gift of ICRF-193.

References

1. Arends, M. J., R. G. Morris, and A. H. Wyllie. Apoptosis: the role of the endonuclease. *Am. J. Pathol.* **136**:593–608 (1990).
2. Ucker, D. S., P. S. Obermiller, W. Eckhart, J. Apgar, N. Berger, and J. Meyers. Genome digestion is a dispensable consequence of physiological cell death mediated by cytotoxic T lymphocytes. *Mol. Cell. Biol.* **12**:3060–3069 (1992).
3. Oberhammer, F., J. W. Wilson, C. Dive, I. D. Morris, J. A. Hickman, A. E. Wakeling, R. P. Walker, and M. Sikorska. Apoptotic death in epithelial cells: cleavage of DNA to 300 and/or 50 kbp fragments before or in the absence of internucleosomal fragmentation. *EMBO J.* **12**:3679–3684 (1993).
4. Oberhammer, F., G. Fritsch, M. Schmied, M. Pavelka, D. Printz, T. Purchio, H. Lassmann, and R. Schulte-Herman. Condensation of the chromatin at the membrane of an apoptotic nucleus is not associated with activation of an endonuclease. *J. Cell Sci.* **104**:317–326 (1993).
5. Beere, H. M., C. M Chresta, A. Alejo-Herberg, A. Skladanowski, C. Dive, A. Kragh-Larsen, and J. A. Hickman. Investigation of the mechanism of higher order chromatin fragmentation observed in drug-induced apoptosis. *Mol. Pharmacol.* **47**:986–996 (1995).,
6. Brown, D. G., X. M. Sun, and G. M. Cohen. Dexamethasone-induced apoptosis involves cleavage of DNA to large fragments before internucleosomal fragmentation. *J. Biol. Chem.* **268**:3037–3039 (1993).
7. Sun, X. M., R. Snowden, D. Dinsdale, M. Ormerod, and G. M. Cohen. Changes in nuclear chromatin precede internucleosomal DNA cleavage in the induction of apoptosis by etoposide. *Biochem. Pharmacol.* **2**:187–195 (1993).
8. Cohen, G. M, X. M. Sun, R. T. Snowden, D. Dinsdale, and D. N. Skilleter. Key morphological features of apoptosis may occur in the absence of internucleosomal DNA fragmentation. *Biochem. J.* **286**:331–334 (1992).
9. Walker, P. R., C. Smith, T. Youdale, J. Leblanc, J. F. Whitfield, and M. Sikorska. Topoisomerase II-reactive chemotherapeutic drugs induce apoptosis in thymocytes. *Cancer Res.* **51**:1078–1085 (1991).
10. Roy, C., D. L. Brown, J. E. Little, B. K. Valentine, P. R. Walker, M. Sikorska, J. Leblanc, and N. Chaly. The topoisomerase II inhibitor teniposide (VM-26) induces apoptosis in unstimulated murine lymphocytes. *Exp. Cell. Res.* **200**:416–424 (1992).
11. Wang, J. C. Recent studies of DNA topoisomerases. *Biochem. Biophys. Acta* **909**:1–9 (1987).
12. Berrios, M., N. Osheroff, and P. A. Fisher. *In situ* localization of DNA topoisomerase II, a major polypeptide component of the drosophila nuclear matrix fraction. *Proc. Natl. Acad. Sci. USA* **82**:4142–4146 (1985).
13. Earnshaw, W. C., and M. S. Heck. Localization of topoisomerase II in mitotic chromosomes. *J. Cell Biol.* **100**:1716–1725 (1985).
14. Earnshaw, W. C., B. Halligan, C. A. Cooke, M. S. Heck, and L. F. Liu. Topoisomerase II is a structural component of mitotic chromosome scaffolds. *J. Cell Biol.* **100**:1706–1715 (1986).
15. Adachi, Y., E. Kas, and U. K. Laemmli. Preferential, cooperative binding of DNA topoisomerase II to scaffold-associated regions. *EMBO J.* **8**:3997–4006 (1990).
16. Cockerill, P. N., and W. T. Garrard. Chromosomal loop anchorage of the *kappa* immunoglobulin gene occurs next to the enhancer region containing topoisomerase II sites. *Cell* **44**:273–282 (1986).
17. Gasser, S. M., and U. K. Laemmli. The organization of the higher-order chromatin loop: specific DNA attachment sites on nuclear scaffold. *EMBO J.* **5**:511–518 (1986).
18. Filipski, J., J. Leblanc, T. Youdale, M. Sikorska, and P. R. Walker. Periodicity of DNA folding in higher order chromatin structures. *EMBO J.* **9**:1319–1327 (1990).
19. Chen, G. L., L. Yang, T. C. Rowe, B. D. Halligan, K. M. Tewey, and L. F. Liu. Nonintercalative antitumour drugs interfere with the breakage-reunion of topoisomerase II. *J. Biol. Chem.* **259**:13560–13566 (1984).
20. Liu, L. F. DNA topoisomerase poisons as antitumor drugs. *Annu. Rev. Biochem.* **58**:351–375 (1989).
21. Herman, E. H., D. T. Witiak, K. Hellmann, and V. S. Waravdeker. Biological properties of ICRF-159 and other related bis(dioxopiperazine) derivatives. *Adv. Pharmacol. Chemother.* **19**:249–290 (1982).
22. Tanabe, K., Y. Ikegami, R. Ishida, and T. Andoh. Inhibition of topoisomerase II by antitumor agents bis(2,6-dioxopiperazine) derivatives. *Cancer Res.* **51**:4903–4908 (1991).
23. Sehested, M., P. Buhl, B. S. Sorenson, B. Holm, E. Friche, and E. J. F. Demant. Antagonistic effect of the cardioprotector (+)-1,2-bis(3,5-dioxopiperazinyl-1-yl)propane (ICRF-187) on DNA breaks and cytotoxicity induced by the topoisomerase II directed drugs daunorubicin and etoposide (VP-16). *Biochem. Pharmacol.* **46**:389–393 (1993).
24. Beere, H. M., J. A. Hickman, R. I. Morimoto, R. Parmar, R. Newbould., and

C. M. Waters. Changes in HSC70 and C-*myc* in HL-60 cells engaging differentiation or apoptosis. *Mol. Cell. Diff.* 1:323–343 (1993).
25. Collins, S. J., R. C. Gallo, and R. E. Gallagher. Continuous growth and differentiation of human myeloid leukaemic cells in suspension culture. *Nature (Lond.)* 270:347–349 (1977).
26. Chung, T. D., F. H. Drake, K. B. Tan, S. R. Per, S. T. Crooke, and C. K. Mirabelli. Characterization and immunological identification of cDNA clones encoding two human DNA topoisomerase II isozymes. *Proc. Natl. Acad. Sci. USA* 86:9431–9435.
27. Jenkins, J. R., P. Ayton, T. Jones, S. L. Davies, D. L. Simmons, A. L. Harris, D. Sheer, and I. D. Hickson. Isolation of cDNA clones encoding the *beta*-isozyme of human DNA topoisomerase II and localisation of the gene to chromosome 3p24. *Nucleic Acids Res.* 20:5587–5592 (1992).
28. Kohn, K. W., L. C. Ericson, R. Ewig, and C. A. Friedman. Fractionation of DNA from mammalian cells by alkaline elution. *Biochemistry* 15:4629–4637 (1976).
29. Dive, C., C. D. Gregory, D. J. Phippe, D. L. Evans, A. E. Milner, and A. H. Wyllie. Analysis and discrimination of necrosis and apoptosis (programmed cell death) by multiparameter flow cytometry. *Biochim. Biophys. Acta* 1133:275–285 (1991).
30. Earnshaw, W. C. Nuclear changes in apoptosis. *Curr. Opin. Cell Biol.* 7:337–343 (1995).
31. Ishida, R., T. Miki, T. Narita, R. Yui, M. Sato, K. R. Utsumi, K. Tanabe, and T. Andoh. Inhibition of intracellular topoisomerase II by antitumor bis(2,6-dioxopiperazine) derivatives: mode of cell growth inhibition distinct from that of cleavable complex-forming type inhibitors. *Cancer Res.* 51:4909–4916 (1991).
32. Kaufmann, S. H., S. Y. Desnoyers, Y. Ottaviano, N. E. Davidson, and G. Poirier. Specific proteolytic cleavage of poly(ADP-ribose) polymerase: an early marker of chemotherapy-induced apoptosis. *Cancer Res.* 53:3976–3985 (1993).
33. Schroter, M., M. Peitsch, P. Gallant, E. A. Nigg, and J. Tschopp. Activation of cdc2 precedes lamin breakdown during apoptosis allowing DNase I to enter the nucleus and leading to DNA breakdown, in *Molecular Basis of Immunology*. European Network of Immunology Institutes (ENII), Les Embiez, France, (1994).
34. Peitsch, M. C., B. Polzar, H. Stephan, T. Crompton, H. R. MacDonald, H. G. Mannherz, and J. Tschopp. Characterization of the endogenous deoxyribonuclease involved in nuclear DNA degradation during apoptosis (programmed cell death). *EMBO J.* 12:371–377 (1993).
35. Fearnhead, H. O., J. A. Rivett, D. Dinsdale, and G. M. Cohen. A preexisting protease is a common effector of thymocyte apoptosis mediated by diverse stimuli. *FEBS Lett.* 357:242–246 (1995).
36. Bruno, S., P. Lassota, W. Giaretti, and Z. Darzynkiewicz. Apoptosis of rat thymocytes triggered by prednisolone, camptothecin or teniposide is selective to G_0 cells and is prevented by inhibitors of proteases. *Oncol. Res.* 4:29–35 (1992).
37. Weaver, V. M., B. Lach P. R. Walker, and M. Sikorska. Role of proteolysis in apoptosis: involvement of serine proteases in internucleosomal DNA fragmentation in immature thymocytes. *Biochem. Cell. Biol.* 71:488–500 (1993).

Send reprint requests to: Prof. John A. Hickman, Cancer Research Campaign Molecular and Cellular Pharmacology Group, School of Biological Sciences, G.38, Stopford Building, Oxford Road, University of Manchester, Manchester, UK M13 9PT. E-mail: john.hickman@man.ac.uk